Astron. Astrophys. 308, 588–600 (1996)

ASTRONOMY
AND
ASTROPHYSICS

Formation of the nebular complex N 11 in the Large Magellanic Cloud*

M. Rosado[1], A. Laval[2], E. Le Coarer[3], Y.P. Georgelin[2], P. Amram[2], M. Marcelin[2], G. Goldes[4], and J.L. Gach[2]

[1] UNAM, Apdo Postal 70-264, 04510 Mexico, DF
[2] Observatoire de Marseille, 2 Place Le Verrier, F-13248 Marseille Cedex 04, France
[3] Observatoire de Grenoble, BP. 53X, Grenoble Cedex, France
[4] Observatorio Astronómico de Córdoba, Laprida 854, 5000 Córdoba, Argentina

Received 15 February 1995 / Accepted 31 August 1995

Abstract. N 11, the second largest nebula of the LMC, is formed of a large bubble surrounded by 9 bright nebulae and filaments. We have observed this nebular complex with a scanning Fabry-Perot interferometer at Hα and [OIII] 5007 wavelengths. The kinematics of this field agrees with the results of the stellar content and of the molecular studies, and shows that such a structure can be the consequence of a sequential star formation. The elements of this result are deduced from the energetic input inside the ionized gas by the stellar winds of the associations LH9 and LH10. The evaluated dynamical lifespan of small nebular entities associated with the more massive stars of LH10, are found significantly shorter than for the gas ionized by the association LH9.

Therefore sequential star formation can be triggered at the shock boundaries of the nebula excited by an OB association in a time scale shorter than previously found, and of at most a few 10^6 yrs. It thus leads to the evidence for a new class of giant bubble, designated as "ring of HII regions" bubble with several distinctive characteristics. It is discussed that the bubbles of this type are formed by sequential star formation over time scales shorter than previously found for some superbubbles.

Key words: ISM: bubbles; N 11 (LMC); kinematics and dynamics – Magellanic clouds

1. Introduction

Bubbles and superbubbles are seen in several external galaxies and in our own Galaxy. They are important tracers of the relationship between stars and gas in the host galaxy by means of powerful winds ejected by massive stars, SN explosions, star formation processes, star photoionization and possibly, cloud collisions. While the formation mechanisms of small bubbles (diameters smaller than 30 pc) are more or less understood, intermediate and large diameter bubbles and even, large HII complexes, could have several possible origins, most of them related to the different degrees of evolution of their initial stellar cluster and to the different environmental conditions. Classically, the intermediate and large diameter bubble formation process has been explained by the combined action of stellar winds and SN explosions of the massive stars belonging to rich clusters inside the bubble (Tenorio-Tagle 1988). This picture has been recently strengthened by the detection of SN signatures inside large HII complexes. However, another tempting mechanism is the sequential star formation, i.e., the "expansion" of star forming fronts triggered by the evolution of a first generation of stars at the center of the present bubble. There are some controversial examples of the action of this latter mechanism (Dopita et al. 1985 and Bormans et al. 1991 for the Shapley III Constellation, Laval et al. 1992 for the N120 HII complex, Walborn & Blades, 1987, and Hyland et al. 1992 for 30 Dor, all of them in the LMC, Lortet & Testor, 1988 for the complexes N158 and N144 in the LMC, and N83-84-85 in the SMC), whereas it has been invoked to explain even the formation of spiral patterns in the LMC (Smith et al. 1987). This controversy is due to the fact that, in general, the time-scales involved in the formation of the new generation of stars at the periphery of the bubble imply the dissolution of the initial stellar cluster at the center so that even if one can ascertain the young age of the clusters at the boundaries, one cannot say anything about the age of the stars at the center. In addition, often the unique evidence for the existence of a triggering shock is the existence of the bubble, as other traces of the formation of these shocks such as SNR characteristic emission or action of stellar winds on the gas have already disappeared.

An inspection of the morphology, kinematics, and stellar content of several bubbles in our Galaxy and in the Magellanic Clouds (Rosado 1984) leads us to think that the formation of

Send offprint requests to: A. Laval

* Based on observations collected at the European Southern Observatory

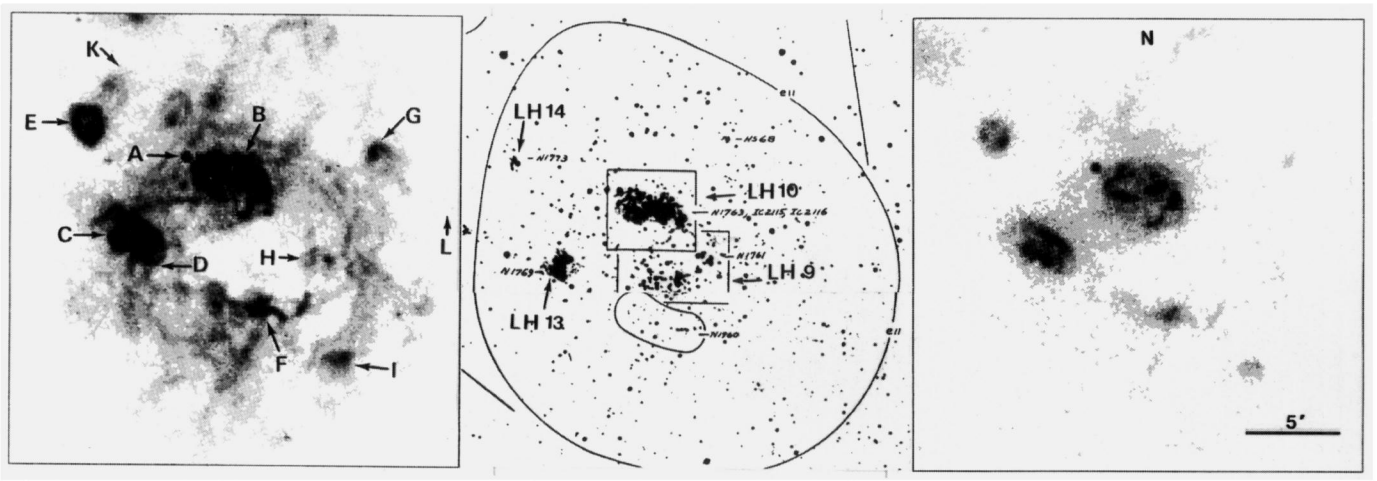

Fig. 1. Monochromatic maps of N 11 A to L, reconstructed from the kinematical frames. The scale is the same for each map. North is up. From left to right: Hα emission; V maps (Hodge & Wright1967) with the positions of the stellar associations; [OIII] 5007 emission.

Table 1.

Region	Stellar Association	Number of stars	Stars of known spectral types (1)	Spectral types (2)	E(B-V)
N 11 E	LH 14 (NGC 1773)	6	Sk 43-66	O 4-5 V	
			-	O 7-8 V	0.22
			-	other exciting stars to the South	
N 11 A	-	-	PGMW 3264	O 3-6 V protostellar cocoon	0.25
N 11 B	LH 10 (NGC 1763, IC 2115,16)	21	Sk 33-66 (PGMW 3209)	O 3 III (f*)+OB	
			PGMW 3168	O 7 II (f)	0.17
			PGMW 3224	O 6 III	
			BI 42 (PGMW 3223)	O 8.5 IV	
			PGMW3061	O 3 III (f)	
			PGMW 3053	O 5.5 I-III (f)	
			BI 39 (PGMW 3157)	BC1 Ia	
				+2 O 9.5 III + +1 O 9.5:IV:+ +3 OV ((f*))+ +11 OV + B stars	
N 11 C	LH 13 (NGC 1769)	10	Sk 41-66	Tight stellar cluster integr. sp. O_5V (>12 massive stars)	0.18
			Wo 599	O 3-O4 V smaller cluster to the South	0.7
Central hole	LH 9 (NGC 1760)	44	Sk 28-66 (HD 32228, Br9,PGMW 1210)	WC 5-6 + +O 9.5 II	0.05
				2 OIa + +3 OIII+OIV+ +13 OV+ 2BIa +15B stars	

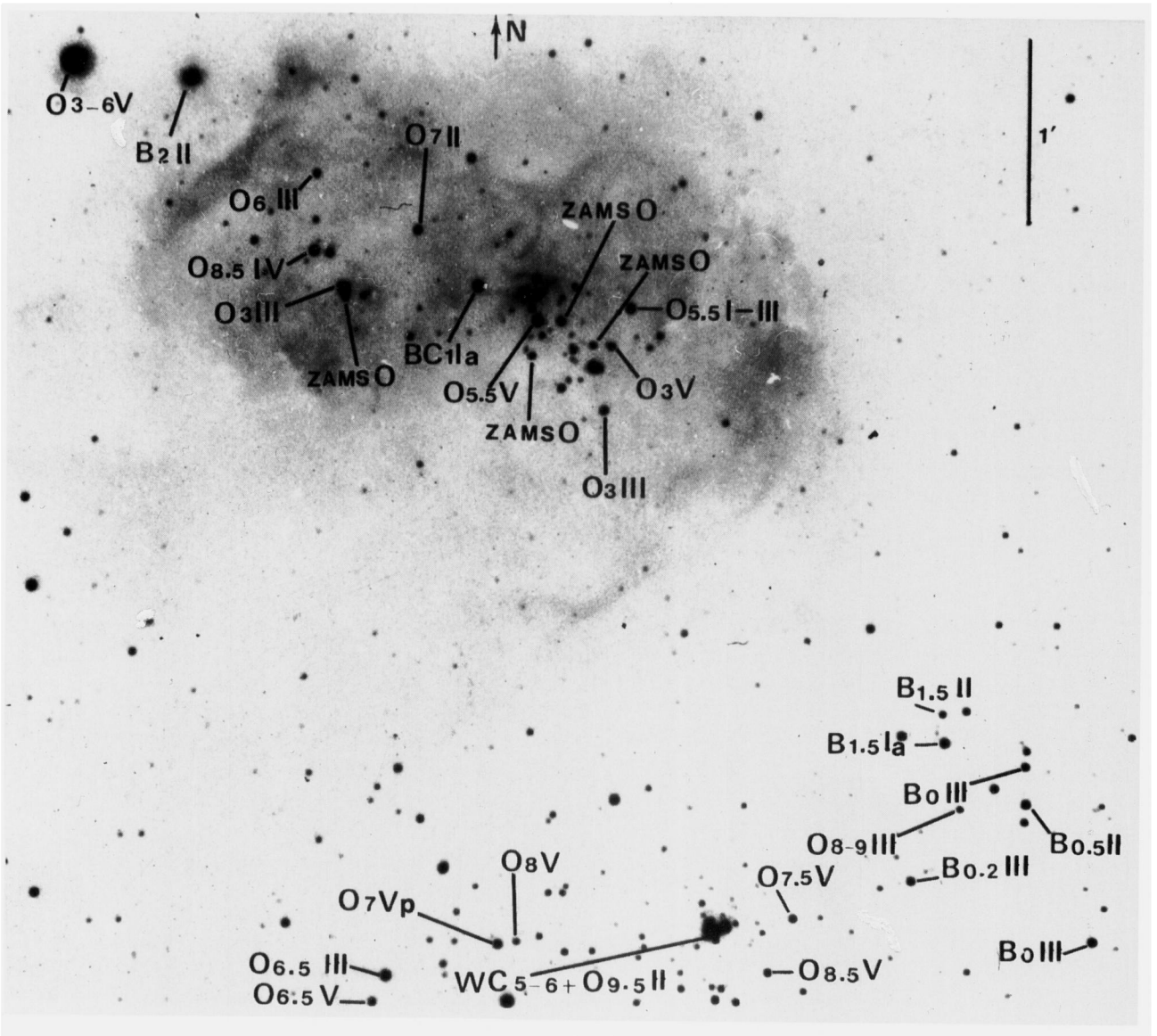

Fig. 2. Positions of the bluest and more luminous stars of the association LH10 at North, and part of the association LH9, seen on a R photograph by Heydari-Malayeri & Testor. The spectral classifications are by Parker et al. 1992.

bubbles of intermediate and large diameters is not due to a single mechanism; it is reflected in differences amongst the properties of these nebulae, as well as of their environment. In this context, we have studied several bubbles in the Large Magellanic Cloud because of its advantages of globality and proximity (Rosado et al. 1990, Laval et al. 1992). Moreover the stellar populations of the Magellanic Clouds have been extensively studied. Very blue stars have been identified; a few stars ought to be embedded inside the gas clouds to explain the observed nebular excitation. On the other hand, the kinematic studies have revealed that some nebulae have violent motions whereas others do not and, in the case of the detection of those motions, the pattern could be very different from one nebula to another. A systematic survey with high spectral resolution should allow to map globally violent motions in the LMC nebulae and to determine the proportion of such detections among the HII regions (i.e. with supersonic motions) of this galaxy.

Such a program of investigation would be tremendous without two-dimensional spectroscopic observations. It has been possible thanks to the Hα survey instrument (Le Coarer et al. 1992). Such a survey has already been completed for the SMC (Le Coarer et al. 1993a and b). It is now in progress for the LMC, and we present here the results concerning the study of gas motions inside the bright cores of the nebular complex N 11. The observations are described in Sect. 2. In Sect. 3 we attempt to understand the relationship between the different smaller nebulae, and to confirm their real membership to this complex by means of their kinematics. Then we precise the types of the different nebulae and their main properties, and we try to determine how they are formed (Sect. 4).

2. The observations

An Hα survey of the Magellanic Clouds and of the Milky Way is being carried out at the European Southern Observatory, at La Silla, with a 36 cm diameter telescope. A scanning Fabry-Perot interferometer is attached to a focal reducer and is equipped with a 2-D photon counting system. We refer to Amram et al. 1991, Le Coarer et al. 1992, and Georgelin et al. 1994, for detailed description and reduction explanations. The Fabry-Perot interferometer, having a spectral sampling of 16 km s^{-1} at Hα and a free spectral range of 376 km s^{-1}, has a coating optimized for transmission not only at Hα, but also at Hβ and at the nearby blue lines such as [OIII] lines. Since the bright nebulae of the LMC produce informative [OIII] emission, the instrument was adjusted to the line [OIII]5007 in the LMC, using a transmission filter centered on the wavelength 5012.4 Å, and calibrated by the line HeI 5015.678 Å. The obtained spectral sampling for the [OIII]5007 observations is 8 km s^{-1} and the free spectral range is 287 km s^{-1}. In the following, the kinematics has been determined by the use of the [OIII] observations, unless otherwise has been specified, and the fluxes are determined by using the Hα observations.

3. The complex N 11

The HII complex N 11 (Henize 1956) or DEM 34 (Davies, Elliott & Meaburn 1976) is the second largest complex in the LMC, after the 30 Dor Nebula; thus it is intermediate between the Giant HII regions (GEHRs) and the classical HII regions. Figure 1 shows our Hα and [OIII] images (obtained by integrating our kinematic frames pixel per pixel) of the complex N 11, which has (at faint levels of the Hα emission) an elliptical shape of 25'.5 x 21' (413 pc x 340 pc at an adopted distance to the LMC of 55 kpc). Several nebulae, filaments and voids are seen forming the complex: first a hollow bubble (hereafter called central hole following Meaburn et al. 1989) surrounded by several filaments and by the bright cores N 11 B and C, the knots N 11 A and D, and the weaker HII regions N 11 F and I. Other HII regions are seen farther away from the central hole: N 11 E and G. The position of the SNR N 11 L is indicated at the very Western part of our Hα image. A comparison between Figs. 1a and c shows that the regions of highest excitation are, by decreasing order, the nebulae N 11 A, B, C, D, E, F and I while, in particular, the central "hole" does not show any detectable [OIII] emission.

The stellar content of this complex is quite rich. The interior stars are found distributed in several associations catalogued by Lucke & Hodge (1970): LH 9, 10, 13 and 14 (Fig. 1b). The individual stars of some of these associations have been studied by Heydari-Malayeri and collaborators in a series of articles (Heydari-Malayeri & Testor 1983, 1985, Heydari-Malayeri et al. 1987). The stars of LH 13 form tight associations of massive stars in such a way that even apparently single stars of LH 13 have been resolved into several components. This is the case of the "star" SK 41-66 which has been recently resolved into more than 12 massive stars (Heydari-Malayeri & Beuzit 1994).

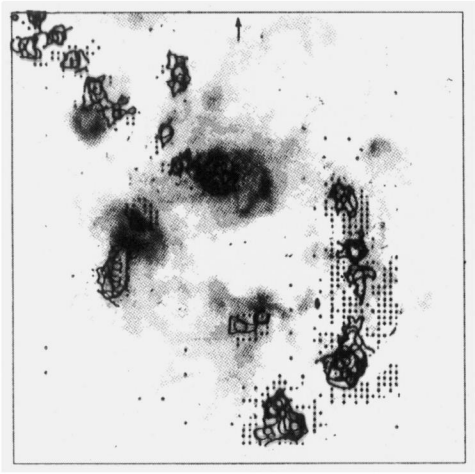

Fig. 3. CO distribution (Israel & de Graauw 1991) superimposed onto an Hα map of N 11.

LH 9 and LH 10 have been studied by Parker et al. (1992). These authors have given arguments suggesting that the ages of the associations LH 9 and LH 10 are different, LH 10 being of more recent formation than LH 9. The recent detection of a methanol maser in the direction of the HII region excited by LH 10 (Ellingsen et al. 1994), is an additional indication that star formation is still going on in this association.

In Fig. 2 we have marked the spectral classifications by Parker et al. (1992) for the intrinsically most luminous blue stars of associations LH 9 and LH 10 from a photograph kindly supplied by Heydari-Malayeri & Testor. Table 1 presents the massive stars identified until now, which are embedded in the different nebulae forming N 11; the stars are named from the catalogues of Sanduleak (1969), Brunet et al. (1975), and Parker et al. (1992). The spectral types and color excesses are found as explained hereafter in the detailed study of each nebula.

N 11 is linked to a large molecular cloud complex, which consists of some 21 separate CO clouds (Israel & de Graauw 1991) distributed in close similarity with the Orion molecular cloud complex. Figure 3 shows that the Southern CO clouds are correlated with a network of Hα filaments surrounding the association LH 9, and forming a shell at the boundary of the central hole.

Figure 4 shows the radial velocity profiles of some selected HII regions of this complex, obtained from the observations described in Sect. 2. Table 2 gives a summary of the main characteristics of all these nebulae, except for N 11 B which is presented in Table 3. We have quoted the dimensions of the region, obtained from our Hα or [OIII] frames, the Hα flux (F(Hα)) of the entire region or some of its velocity components, taking as flux calibrators the HII regions measured photoelectrically by Caplan & Deharveng (1985). Then we correct the flux for interstellar extinction according to the values given in Table 1, and we calculate the emission measure (EM) and the rms electron density (ne) in the same way as for the N120 complex (see relations 1 and 2 and discussion of Sect. 5 of Laval et al. 1992). The rms electron density has been evaluated by assuming an

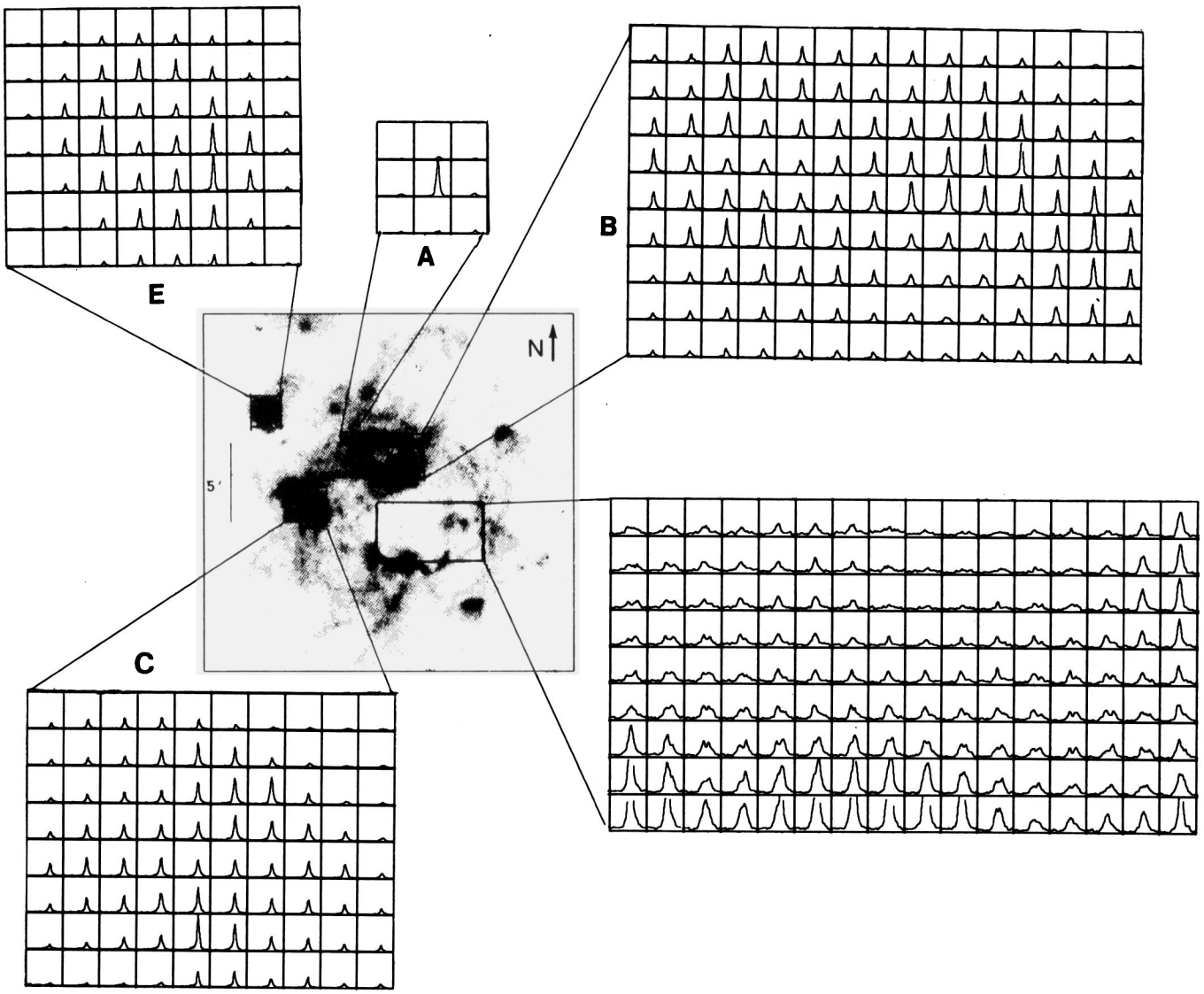

Fig. 4. Examples of the radial velocity profiles of the nebulae N 11 A, B, C, E and central hole. Every profile is obtained over an area of 18" x 18" covering 4 pixels.

homogeneous sphere of diameter D (case a) or a spherical shell of diameter D and thickness D/24 (case b). We have also quoted in Table 2 kinematic quantities obtained from our data such as: the heliocentric systemic velocity (V_{sys}) the velocity components of the split profile (if any), the FWHM corrected from the instrumental function of the different components and an estimate of the nebular expansion velocity (V_{exp}) for the complex velocity profiles. This latter quantity has been defined as the velocity difference between the average velocity of the associated HII region and the most positive or negative velocity of the components (Chu & Kennicutt 1988). In the case of supersonic motions we have also quoted an estimate of the kinematic age of the nebula defined as $t = 0.6\ R/V_{exp} \times 10^6$ yr.

In what follows, we will review each part of N 11, separately, going from East to West and from North to South.

3.1. The nebula N 11 E

The dimensions of N 11 E that we observe in the [OIII] emission are 126" x 135" (34 pc x 36 pc). In Table 1 we have quoted the stellar content of this HII region based on the work of Heydari-Malayeri et al. (1987). The reported stars belong to the association LH14 (NGC 1773). Our data show no splitting over the map of the line profiles of the [OIII] emission (Fig. 4), which are well fitted by pure Gaussians, with a very small FWHM (Table 2). Thus no measurable expansion of the gas exists over dimensions equal, at least, to our spatial resolution of 9".

3.2. The nebula N 11 A

This region has been studied by Heydari-Malayeri & Testor (1985). The emission of the blob N 11 A presents the sign of a bright, highly excited HII region, though its exact nature is

Table 2.

	Dim (pc)	Hα Flux x10^{-10}erg cm^{-2} s^{-1}	E.M. cm^{-6}pc	n_e (rms) cm^{-3}	V_{Sys} (helio) km s^{-1}	Velocity comp. km s^{-1}	FWHM km s^{-1}	V_{exp} km s^{-1}	Kin. age year
N 11 E	34x36.5	1.136	5645	12.7 case a)	278	Single	10	-	-
N 11 A	1.5x1.5	0.17	10795	184 case a)	284	Single	18	-	-
N 11 C	49x34	4.493	14915	19 case a)	288	Single	16	-	-
Central Hole	97x97	1.6	640	7.7 case b)	285	285	24		
1^{rst} comp.								V_R-V_{HII}	2.5 x 10^6
2^dcomp.		0.36	150	3 case b)		330	-	45	
SNR						100	-	V_{HII}-V_B	
	16x24	0.07			289		-	190	1.1 x 10^4
N 11 L						> 630	-	V_R-V_{HII} >350	

not clear; it looks like a spherical knot of 12" diameter (3.2 pc) with the highest [OIII]/Hα line-ratio in N 11. The extinction is found to be normal, and the excitation source should be at least one ZAMS star of Teff = 44000 K. Parker et al (1992), after discussion, incline for a O3-6 V star, "beginning to emerge from its protostellar cocoon". Our spatial resolution of 9" does not allow a detailed investigation of this knot. Our [OIII] data give an indication of a relatively quiet gas as the line profiles do not show any sign of splitting (Fig. 4). Thus if an expanding motion greater than 10 km s^{-1} exists inside N 11 A, it is not developed over dimensions longer than 9". Kinematic studies at better angular resolution are highly encouraged.

3.3. The nebula N 11 B

N 11 B is a nebula of 252" x 216" (67 x 58 pc), having a sharp increase of intensity at the Northern, Eastern and Western edges. Some filaments progressively decreasing in intensity can only be seen to the South West. It is interesting to note that, as regards to the coordinate position, the bigger CO cloud is seen superimposed to N 11B, and that the CH_3OH maser seems to be laying midway between the stars PGMW 3209 and 3061 (Parker et al. 1992) embedded in N 11B. This bright nebula surrounds the stellar association LH 10 (NGC 1763, IC 2115, 16), which is studied by Heydari-Malayeri et al. (1983) and Parker et al (1992). The latter authors found that LH10 seems to be the youngest association embedded inside N 11, with ongoing star formation (see Sect. 3), and that it presents a peculiar IMF for the LMC, flatter than usually. The stars are not concentrated at the center of the association (Fig. 2), but instead, they are separated giving rise to several smaller nebulae probably associated with individual stars. We can disentangle six small nebulae, by kinematic means, because some of them undergo

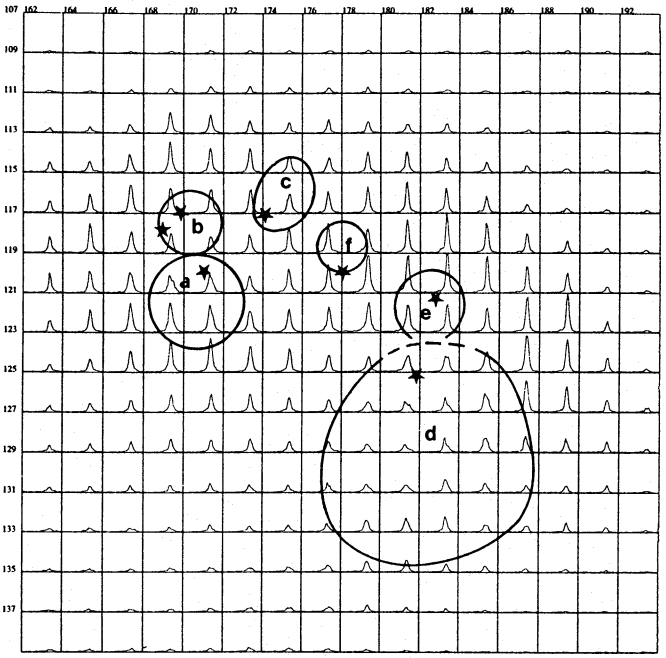

Fig. 5. Identification of six nebular entities inside N 11B, from their radial velocity profile. The profiles are integrated over 18" x 18" squares.

moderate expansion motions. These nebulae are designated as a) to f) in Fig. 5. The average heliocentric radial velocity of the whole nebula N 11 B is 292 km s^{-1} (FWHM = 23 km s^{-1}). Several physical parameters of these small nebulae, obtained from our observations, are given in Table 3.

Table 3 reports observational characteristics of these different regions such as angular dimensions of the split area (the

kinematics cannot give information upon the thickness of the exterior shocked layer), average heliocentric velocities, FWHM and signal/noise ratios (S/N) of the different components. It quotes also several quantities derived from the observations: the difference of velocities between the whole HII region N 11 B and the component, either red (R) or blue (B), the estimated rms electron density of each component, an estimate of the kinetic energy (KE) involved in the motion of each component, the earliest spectral type of the ionizing stars, and the kinematic age of the nebula in the case of detection of supersonic motions.

The rms electron density of each component has been obtained in a different way than described in Sect. 3. The Hα flux of the entire N 11B nebula has been measured by Caplan & Deharveng (1985) within a 4'.89 diaphragm, which includes not only N 11 B but also some fainter emission to the North and to the South. They obtain a value of 8.967 10^{-10} erg cm^{-2} s^{-1}. Our kinematic information at Hα allows only to calculate the Hα fluxes of the Eastern and Western regions of N 11B. The corresponding values are 1.13 10^{-10} and 0.782 10^{-10} erg cm^{-2} s^{-1} respectively. On the other hand the splittings reported in Table 3 have been obtained from the [OIII] kinematics (the Hα profiles give the same mean velocities, but they are too broad to show any splitting). In order to calculate the relative Hα fluxes of the split components, we have assumed that the [OIII] intensity of each component is proportional to the corresponding Hα intensity. Thus, these flux values are highly uncertain. The rms electron densities of the different components have been obtained from these fluxes, corrected from the interstellar reddening reported in Table 1 and by assuming that the nebula is homogeneous. We have identified the velocity difference, V_{HII} - $V_{B/R}$, with the expansion velocity. The kinetic energy, 1/2 M_{comp} V^2_{exp}, has thus all the uncertainties related to the rms electron density, the expansion velocity and adopted lower limits for the dimensions of the nebulae. On the other hand, since the ambient medium contains neutrals and molecules, the kinetic energy derived at optical wavelengths, could be only a small fraction of the kinetic energy imparted to the other components. In the following, the characteristics of the 6 regions inside N 11B are described. The stars studied by Parker et al. (1992) are indicated by their number preceded by PGMW.

a) The zone N 11Ba is associated with the O3 III (f) star PGMW 3209. This zone is wide enough to allow precising the gas motion: the fastest and brightest splittings occur just south of the star 3209, with components at 283 km s^{-1} (S/N = 50, FWHM = 18 km s^{-1}) and 310 km s^{-1} (S/N = 23, FWHM = 18 km s^{-1}). The high flux suggests a huge amount of moving gas; the amplitude of the gas motions detected inside such a dense nebula of the LMC, is rather rare, except in 30 Dor. No bubble is visible though the stellar wind should be very powerful; the star PGMW 3209 is one of the three O3 earliest-type stars of N 11, found by Parker et al. (1992).

b) The zone N 11Bb is associated with the two neighboring stars PGMW 3224 and 3225 of respective spectral types O6III and O8.5IV. The amount of moving gas is also substantial, and equivalent for both velocity components. All around the nebula boundaries, only one component profile is present, with a velocity equal to 291 km s^{-1} (S/N from 75 to 100, FWHM from 16 to 19 km s^{-1}).

c) The zone N 11Bc is situated north from the star PGMW 3168 which is an O7II (f) star. South of the star, the line profile is purely Gaussian.

d) The zone N 11Bd is associated with the star PGMW 3061 of spectral type O3III (f). Its dimensions, with respect to the star position, are as far as 18" North, 18" West, 45" East and 54" South where the emission decreases.The kinematics reveals the maximum splitting of the radial velocity profiles to be at the position of the star, with components at 282 km s^{-1} (S/N = 23 and FWHM = 18 km s^{-1}) and 315 km s^{-1} (S/N = 9 and FWHM = 18 km s^{-1}). The intensity of the two components decreases from North to South; moreover the line profiles become more complex towards the South (Fig. 5), suggesting the presence of other faint components.

Two other blue supergiant stars appear to drive gas motions around them, but with much fainter high velocity components; their zones of influence are:

e) The zone N 11Be in the direction of the star PGMW 3053 (spectral type O5.5I-III(f)). North of the star, one of the small components is still present with 256 km s^{-1} (S/N = 3, FWHM = 13 km s^{-1}) while the 296 km s^{-1} component has S/N = 92, and FWHM = 13 km s^{-1}.

f) The zone N 11Bf, at the position of the star PGMW 3157 (spectral type BC1Ia); to the north the profile has one major component at 292 km s^{-1} (S/N = 67, FWHM = 16 km s^{-1}), and two small wings at 251 and 322 km s^{-1} both with S/N = 3 and FWHM = 16 km s^{-1}.

As one can see from Table 3, such values of the expansion velocities and their simultaneous existence make it unrealistic that their origin could be undetected SN explosions. From the above properties, it seems plausible that stars PGMW 3053 and 3157 have already dissipated their own environmental gas, at least partially, or that they are situated in a less dense part of the nebula and of the original cloud. Even with the high uncertainties involved in the estimation of the kinetic energy, the obtained value agrees with the spectral type of the exciting star in the sense that the larger the kinetic energy, the earlier the stellar spectral type. However, the estimated kinetic energy is at least a factor of 10 smaller than the kinetic energy that can be supplied either by the stellar radiation or by the stellar winds of these early-type stars (in this latter case, 4 x 10^{48} ergs = 20 % of 2 x 10^{49} ergs for a mass-loss of 10^{-6} $M_\odot$, wind velocity of 2000 km s^{-1} during 5 10^5 yr, taking this last value as a typical kinematic age of the nebulae according to Table 3). Taking into account the uncertainties in the diameters and rms electron densities, and the possibility of motions of neutrals and molecules, the estimates of the kinetic energy deduced from optical observations indicate that the wind-blown bubble origin is highly probable. Furthermore, the detected supersonic motions present in most of these nebulae, are more in agreement with the action of supersonic winds than with the stellar radiation models. Thus, we think that we are detecting individual entities inside a larger nebula, driven by the stellar wind of the individual exciting stars.

Table 3.

Region	Dim. Diam (pc)	V_{hel} comp. km s^{-1}	S/N	FWHM km s^{-1}	$V_{R/B}$-V_{HII} (km s^{-1})	n_e(rms) (cm^{-3})	K.E. (x10^{47} ergs)	Earlier sp. type	$t_{kin.}$ = 0.6 R/V
N 11 Ba	54"x36"	283	55	20	-9	19	3.5	O_3III	2.6 10^5
	12	306	29	20	+14	10	4.4		
N 11 Bb	(36"x18")	285	36	17	-7	17	0.6	O_6III	
	8.5	299	38	14	+7	20	0.7		
N 11 Bc	(27"x27")	296	45	18	-14	16	1.5	O_7II (f)	1.6 10^5
	7.5	278	27	14	+4	23	0.18		
N 11 Bd	54"x90"	283	33	18	-10	5	4.6	O_3III (f)	3.9 10^5
	19.5	308	20	18	+15	5	10		
N 11 Be	(27"x18")	296	105	11	(-35)	3	(1.0)	$O_{5.5}$I-IIII (f)	
	6	(326)	8	14	(+33)	4	(1.2)		
		(258)	5	14					
N 11 Bf	(18"x18")	283	72	7	-10	14	0.21	BC_1Ia	1.5 10^5
	5	(331)	5	8	(+38)	4	(0.85)		

3.4. The nebula N 11 C

N 11 C has been studied by Heydari-Malayeri et al. (1987) who identified the star Wo 599, an O3-O4 V star, as one of the ionizing sources of N 11 C, in addition to the cluster Sk-66 41. The latter, previously considered one of the most luminous stars in the LMC, is found now to be a tight cluster of more than 12 massive stars (see Sect. 3). All these stars are members of the stellar association LH13 (NGC 1769) which contains at least 15 additional blue stars. High angular resolution images of the inner stars and the high excitation of the associated nebula N 11 C point towards the existence of additional massive stars inside N 11 C. Some of the best candidates which could contribute to the excitation are the stars of the small cluster situated close to the southern boundary of N 11 C, where the [OIII] emission is increasing. N 11 C is also a well defined nebula, of 180" x 126" (49 pc x 34 pc). The [OIII] emission, bright in the central parts, decreases progressively towards the boundaries, as the Hα emission does. No evidence of a bubble or a ring can be seen. The [OIII] profiles are Gaussian, without splitting, even near the O3 V star and near the bright stellar cluster Sk-66 41, where the radial velocity is 286 km s^{-1} with a FWHM of 14 km s^{-1}. Nor does the gas close to the fainter southern cluster show any sign of splitting; however the radial velocity is slightly different there, with 291 km s^{-1} (FWHM = 14 km s^{-1}). As for N 11 A and N 11 E, no expansion higher than 10 km s^{-1} occurs now inside N 11 C over dimensions of at least 2.2 pc.

3.5. The central hole and the nebula N 11 F

3.5.1. Morphology of the emission

This region, of 6' (97.2 pc) in diameter, has been studied by Meaburn et al. (1989). In the faint emission over the central hole, they detect up to 5 separate velocity components, covering a range of heliocentric radial velocities from 210 to 370 km s^{-1}. Meaburn et al. (1984) have searched for HI layers in this direction and have found only single 21 cm profiles at V_{hel} = 289 $\pm$ 2 km s^{-1}. The ionizing stars belong to the OB association LH 9 (NGC 1760). Parker et al. (1992) detailed the stellar content of LH9 which contains one WC star, 3 supergiants Ia, 6 stars of luminosity classes II and III, numerous O6 dwarfs, and several stars of later types, (see Table 1 and Fig. 3). The slope of the IMF found by Parker et al. (1992) is normal. The southernmost filament of N 11 B defines the northern boundary of the central hole (Fig. 1); the southern boundary of the hole is defined by N 11 F, which is weakly emitting in [OIII]. Between them, no [OIII] emission is detected. This is quite surprising since a WC5-6 star (HD32228) belongs to the stellar cluster. As emphasized by Meaburn et al. (1989), the Hα emission is also very faint on the line of sight of LH9, showing that the gas density may be very low there, while the extinction is smaller than for the association LH10. On the other hand, no sign of explosion of a supernova has so far been detected inside this hole. Towards the boundaries, mainly to the West, the emission increases showing circular filaments (3' to the West of HD 32228, S/N=43). 1'.8 to the North and 5'.25 to the East of HD 32228, the faint nebular emission encounters the bright nebulae N 11B and N 11C-D.

3.5.2. Two-D kinematics and rms density

The 2-D kinematics is obtained from the Hα observations. In the following, a S/N ratio of 5 has been considered as the lower limit usable for studying the non-Gaussian velocity profiles. Such a limit is twice higher than the brightest OH night-sky line (6568 Å) transmitted through the wavelength band of the interference filter used. The velocity profiles are rather complicated at the center whereas they are simple at the boundaries of the hole. However, splittings still occur towards the nebula N 11C-D and also inside the minor cavities located to the South and to the West.

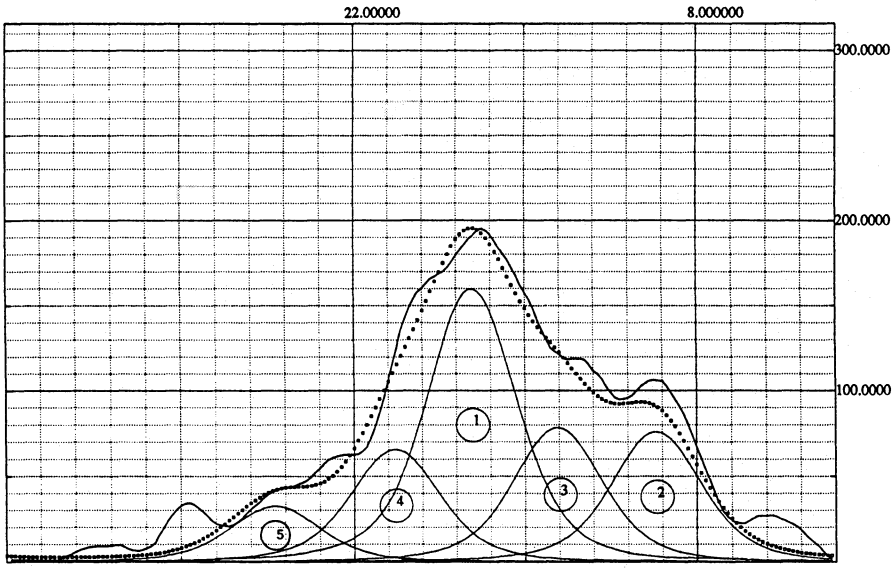

Fig. 6. The multi-component velocity profile of the Hα emission surrounding the WC star of LH9, obtained over an area of 36" x 54"; the night sky emission lines have been subtracted from the profile.

Figure 6 shows the most complex velocity profile in the central hole. It has been obtained from a small region (90" x 90") centered on the WR star. The slit position observed by Meaburn et al. (1989) crosses this region. Five velocity components are necessary to fit the profile: 359 km s^{-1} (S/N=5), 326 km s^{-1} (S/N=3), 275 km s^{-1} (S/N=11), 239 km s^{-1} (S/N=3) and 185 km s^{-1} (S/N=2), the FWHM being 32 km s^{-1} for all components. There is some indication of gas at smaller velocities but near our limit of sensitivity. The average heliocentric radial velocity evaluated over an area of 6'.1 x 3'.1, centered on the association LH9, and not taking into account the gas linked with N 11B, N 11D and N 11F, is 285 km s^{-1} (FWHM= 50 km s^{-1}); moreover, the integrated profile shows a much fainter component at 330 km s^{-1}. The velocity of the main component agrees with the HI velocity of 289 $\pm$ 2 km s^{-1} (Meaburn et al. 1984). The width of the main component and the existence of a second component indicate that high internal motions are covering a large area. Therefore we review the spatial extent of the several components, which is also shown in Fig. 7:

a) Blue components: The component at 185 km s^{-1} is seen only over an area of 1' x 2' surrounding LH9. However, the component at 230-250 km s^{-1} extends as far as N 11F and even further to the South whereas towards the East it reaches the vicinity of N 11C-D, covering an area of 5'.25 x 3'.3 (Fig. 7)

b) Red Components: The 320 and 360 km s^{-1} components are detected over almost all the nebula, sometimes both together but often separately; the intensity of the emission is not uniform; it occurs in small places or in filaments: the Northern filament is particularly outstanding at a velocity of 315 km s^{-1} (Fig. 7), as is also the nebulosity between N 11B and N 11C-D. The only region without any redshifted gas is the area located to the South of N 11C-D. Thus, the region having redshifted material covers 12'.75 x 21'.75, i.e. almost the complete nebular complex N 11 and not only the central hole.

In Table 2 we have quoted an expansion velocity of 45 km s^{-1} obtained from the difference between the systemic velocity (285 km s^{-1}) and the 320 km s^{-1} velocity component. The central hole is obviously linked with the stellar association LH9 containing the WC star HD32228. Indeed, gas motions are more violent near this WR star (see Fig. 6). The velocity profile integrated over an area of 6'.1 x 3'.1 around the WC star shows a bright broad (FWHM = 50 km s^{-1}) component at the systemic velocity of the whole complex, and a much fainter red-shifted component. Meaburn et al. (1989) have indicated that this high velocity dispersion is due mainly to the existence of a cellular structure due to small bubbles expanding with velocities between 20 to 80 km s^{-1}. Our radial velocity field, over the entire central hole area, corroborate this since we also obtain complex velocity profiles in the core and towards the Southern border of the central hole. However, we were able to disentangle that the bulk of the gas motions (traced by the bright velocity components, thus the densest) follows a kinematic pattern which is roughly compatible with a radial spherical expansion. In order to do that, we have obtained integrated velocity profiles over regions of 90" x 90" covering an area of 10'.5 x 6'. This area covers the central hole but avoids the bordering HII regions N 11B and N 11C. It is centered about 1'.5 South of the WC star, thus, including N 11F. We have decomposed the velocity profiles of these regions in their Gaussian components. Figure 8 shows the plot of the radial velocities of the components with S/N $\geq$ 5, obtained this way, versus the distance of the center of the region to the WC star. At distance equal to 0, we have plotted the components of the complex profile shown in Fig. 6, regardless of their S/N ratio. This plot shows that most of the points have a constant velocity component at 292 - 298 km s^{-1} coinciding, (within the uncertainties) with the value of the systemic velocity of the whole complex, already found. The points having this velocity component correspond to the more exterior regions inside the studied area. On the other hand, the regions inside a central rectangle of 7'.5 x 3', show splitting of their velocity profiles in two components: an almost constant velocity component at 272 - 278 km s^{-1} and a redshifted component

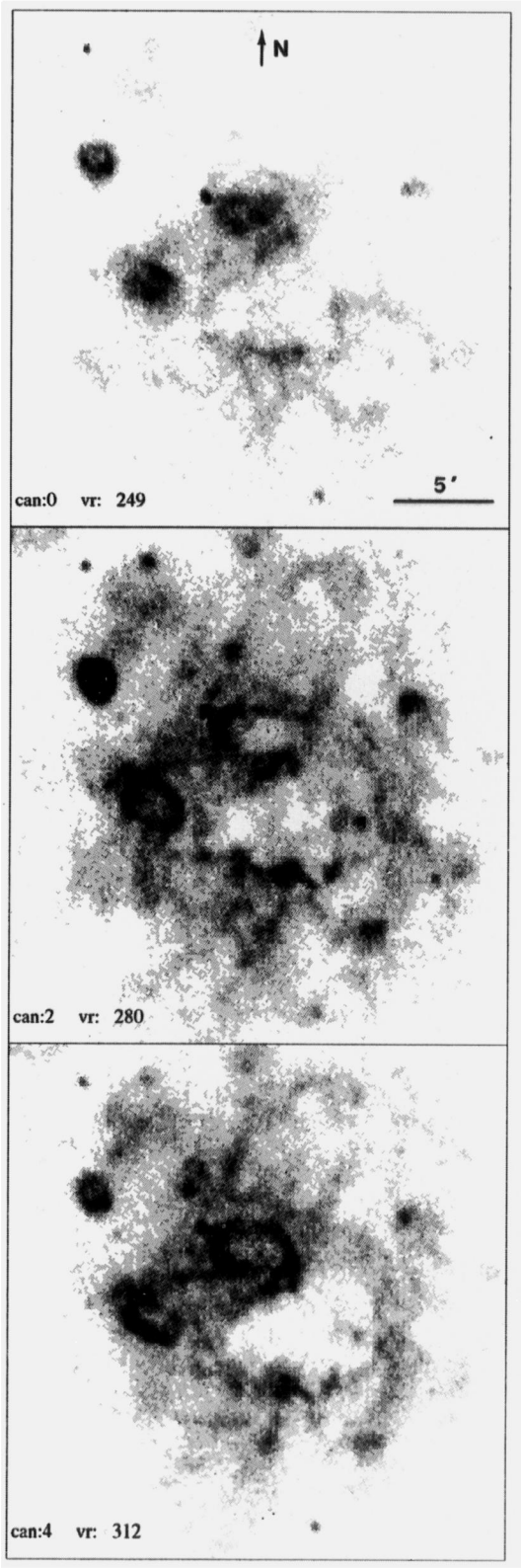

Fig. 7. Wavelength maps of N 11 corresponding to the following heliocentric radial velocity range: 249 ± 8 km s^{-1}; 280 ± 8 km s^{-1}; 312 ± 8 km s^{-1}.

which decrease in magnitude as a function of the distance to the center, as it is expected in a radial expansion. From this plot we find again a value of about 45 km s^{-1} for the expansion velocity of the bulk of the mass forming the central hole. This does not exclude that lower density gas undergoes cellular expansions as discussed by Meaburn et al. (1989).

It is interesting to note that this roughly regular pattern is lost if we extend the area by including the bordering HII regions and the gas interconnecting them. In fact, if we include the velocities of the HII regions which border the central hole, in particular, those of N 11B and the gas to the South of the central hole, we find splitting of the velocity profiles at those bordering HII regions.

From these parameters for the bulk gas motions we can estimate the kinetic energy involved in the motion of this region. Meaburn et al. (1989) have calculated this quantity too. They obtained an estimate of 2.3 x 10^{50} ergs which agree with our own estimate. This energy could be supplied by the stellar winds of the interior stars (Table 1) if the bubble is pressure-driven by the winds. We can examine also the possible role of SN explosions in the formation and energetics of this hole. The typical way to estimate the number of SN in an association is to find the number of stars susceptible to explode as type II SN (B3 or earlier) and then, to estimate the mean time between SN explosions and to compare it with an estimate of the age of the cluster. This method is valid after 5 x 10^7 yr (the lifetime of a 7 $M_\odot$ star). Here, since the dynamical age (2.5 x 10^6 yr) is shorter than 5 x 10^7 yr, we will proceed in a different way taking advantage of the detailed knowledge of the stellar content inside this hole (LH 9) studied by Parker et al. (1992). Indeed, these authors have found that there are 4 stars in the mass bin 40-60 $M_\odot$ which are the most massive stars in this association. Furthermore, they have obtained an "Initial" Mass Function (IMF) with a slope γ = -1.6. This slope is fairly robust because the exclusion of the bins corresponding to the most massive stars (subject to small number statistics) and to the less massive stars (subject to detection bias) does not change the obtained slope by more than 0.15.

If one assumes that only stars more massive than 40-60 $M_\odot$, could have already exploded as SN, one can make an estimate of the number of SN by extrapolating the IMF to higher mass bins. We have done that by assuming an upper limit to the stellar mass of 100 $M_\odot$. Thus, we have calculated the number of stars in the mass bins 60-80 $M_\odot$ and 80-100 $M_\odot$ given the IMF of Parker et al. (1992). We have found that only 3 stars could have been exploded as SN under the assumptions made.

Even if this number is highly uncertain (it assumes that only the more massive stars could have been exploded, that the highest stellar mass is about 100 $M_\odot$, and it is subject to the very small number of massive stars and evolutionary effects), the energy liberated to the ISM from the SN explosions is about 3 x 10^{51} ergs from which 20% is transfered as kinetic energy of the gas: 6 x 10^{50} ergs. This number is highly sufficient to explain the kinematics of the central hole (estimated kinetic energy about 2.3 x 10^{50} ergs) implying that, at those early stages, stellar winds and SN contend in energizing the gas. It is interesting to note

that our estimate of the number of SN present in LH 9 is considerably lower than the estimate made by Meaburn et al. (1989) based on global statistical properties of SNRs and HII regions in the LMC. Nevertheless, no traces of SNR emission have been detected until now, but the indication by Hunter (1994) that the northern emission, outside of the loop, presents higher [SII] /Hα and [NII]/Hα ratios than the other areas of N 11.

3.6. The SNR N 11 L

This SNR appears as a faint small nebulosity at the very western edge of our frames. It is one of the LMC SNRs for which no X-ray emission has been detected. Its spectrum has been studied by Danziger & Liebowitz (1985) who find electron densities between 70 and 300 cm^{-3}. Its morphology and kinematics has been studied by means of an echelle spectrograph by Meaburn (1987) and by Chu and Kennicutt (1988). Meaburn showed that even if the whole body has a systemic velocity of 289 km s^{-1}, the redshifted material has expansion velocities larger than 350 km s^{-1} while the blueshifted gas has an expansion velocity of 190 km s^{-1}; this implies that the red-shifted gas has larger velocities, relative to the systemic motion, than the blue-shifted gas. This is similar to the velocity fields found in some galactic SNRs such as IC443 (Lozinskaya 1979) and G65.2+5.8 (Rosado 1981), where this asymmetry in the expansion velocities of red and blue shifted gas has been attributed to large scale density gradients. Here, the presence of the molecular cloud mentioned in Sect. 3, could create these gradients. Meaburn (1987) gives an upper limit to the age of this SNR of 1.1 10^4 yr. Our data agree with Meaburn's data. Thus, we confirm that it is a member of the N 11 complex (given its systemic velocity) and that its kinematic peculiarities are due to the interaction of high density gas (perhaps the edge of the molecular cloud) with the blast wave. The molecular cloud could be also responsible for the non-detection of soft X-rays from this SNR.

3.7. Other nebulae without known exciting stars

The embedded stars inside N 11 F, G, H and I are unknown. Little or no [OIII] emission is visible, but for N 11 F. The Hα kinematics is quiet, with an intense main emission well fitted by a Gaussian of FWHM = 32 km s^{-1}. The heliocentric radial velocities averaged over N 11 F, G, H, and I are respectively 293 km s^{-1} (S/N = 149), 286 (S/N= 78), 280 (S/N = 41), and 288 km s^{-1} (S/N = 112). The two extended red-shifted components at 320 and 360 km s^{-1} (Sect. 3.5) are the only faint components visible in the foot of the main Gaussian. Such a low-motion pattern and the locations of these nebulae lead to presume that they are condensations ionized by the stars of the association LH 9, except for the nebula N 11 G, which looks to be farther out to the North, unless it is situated at the foreground or at the background of the central hole. These nebulae are not included in Table 2.

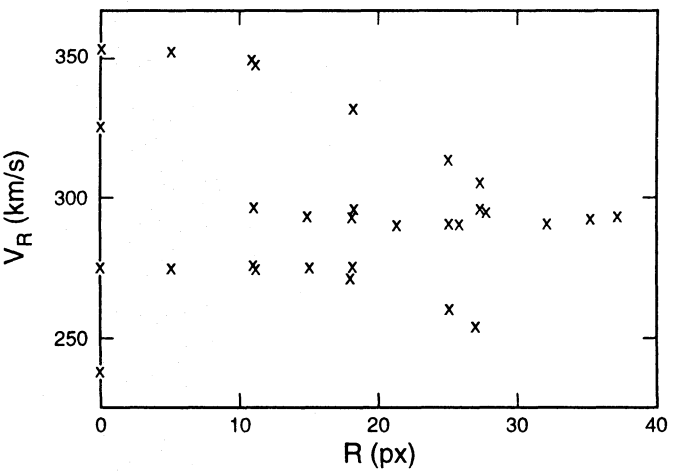

Fig. 8. Plot of the heliocentric radial velocity versus the distance to the centre of expansion (in arbitrary units).

4. Discussion

This nebular complex is, in structure, very similar to the nebular complex N120 previously studied (Laval et al. 1992). Even if N 11 is more than three times larger than N120, both complexes share a series of common characteristics. As in N120, a central hole, with a WC star, can be observed, surrounded by smaller nebulae, more or less coeval, including a SNR and a small, dense HII region (N 11A and N120B). As in the case of N120, evidences are found for a strong association with a molecular cloud. However, while in N120 we were unable to show that this nebular complex is formed by sequential star formation, here we benefit from a better knowledge of the stellar content inside the hole and in all the surrounding nebulae. Indeed, its stellar content belongs to several stellar associations already catalogued by Lucke & Hodge and where the works of Heydari-Malayeri and collaborators (Heydari-Malayeri & Testor 1983, 1985; Heydari-Malayeri et al. 1987; Heydari-Malayeri & Beuzit 1994) and Parker et al. (1992) are of invaluable interest. Though the stars are concentrated in associations (the associations LH9 for the central region, LH 14 for N 11E, LH10 for N 11 A-B and LH13 for N 11C), our study shows that even inside the associations one can discriminate individual nebular entities formed by one or a small number of stars belonging to these associations. This is the case not only for the small HII region N 11A, which is still probably in the cocoon phase, but also for at least 6 nebulae conforming the "complex" N 11B, mainly ionized by Of stars or supergiants, some of them undergoing supersonic expansions up to 38 km s^{-1}. Thus, the interferometric 2-D view shows a necklace structure made of bubbles in formation with kinetic ages of a few 10^5 yr (Table 3). These nebulae are most probably formed by the action of the strong stellar winds of the exciting stars to which they are associated, and a correlation between the kinetic energy of each individual nebula and the spectral type of the exciting star, is found. More sensitive observations with higher angular resolution are required in order to better study these individual nebulae.

On the other hand, the central hole is linked with the stellar association LH9. In Sect. 3.5.2 we have estimated a kinematic age of 2.5 x 10^6 yr. The older kinematic age of the central hole agrees well with its low density gas and its large dimensions. The stellar winds are known to be extremely efficient to evaporate the parental gas. The efficiency increases during the evolution of the star, and can be quantified (Oey & Massey, 1994). The dynamical age of the nebula reflects the age of the powerful wind and indicates the first evolving events in the life of the star. Thus the small bubbles indicate recently evolved stars, and the stars of LH10 should be less evolved than the stars of LH9. The energetic input into the gas leads to deduce that the stars of LH10 were born later than the stars of LH9. It is quite challenging to try to estimate the age of young stellar associations (such as LH9 and LH10) from color-magnitude diagrams (CMDs) and consequently, several other arguments have been given in order to show that LH9 and LH10 are of different ages even if both are young (Parker et al. 1992). One argument is that they are different at least in their triggering star formation mechanism. The discovery of a methanol maser in LH10 (Sect. 3) has corroborated the validity of this conclusion. A similar conclusion can also be deduced from the map of the FIR-to-6.3cm brightness ratio made by Xu et al. (1992). A higher ratio is found at the North-Eastern quarter of N 11 towards LH10, than at the South-Western quarter. So all the different indicators point towards the same conclusion. In the case of LH13 and LH14 there are no similar studies on their IMF. In particular, for LH13, the observational difficulties in obtaining the spectral classification of the 12 components of the tight cluster recently found for Sk 41-66 are quite strong. However, the work of Heydari-Malayeri et al. (1987), complemented with the new results found for Sk 41-66 (Heydari-Malayeri & Beuzit 1994), imply that both associations are quite young and much probably younger than LH9. Indeed, LH13 and 14 share with LH10 some of the properties given by Parker et al. (1992) as indicative of a younger age for LH10 relative to LH9. The appearances of the nebulosities associated with LH13 (N 11C) and LH14 (N 11E) are more similar to N 11B (associated with LH10) than with the shell structure centered on LH9 (the central hole). Even more, as LH10, LH13 and 14 are at the borders of this shell structure. Here also, these differences represent a real difference in the environments of LH13 and 14 and LH9; in fact, the E(B-V) values quoted in Table 1 for all these regions imply that the extinction is at least 3 times higher for LH10, 13 and 14 than for LH9. Additional evidences of the youth of LH13 and 14 are the following: a) Both associations have massive stars with main-sequence spectra. In particular, LH13 has an O3-4V star and a quite tight cluster of massive stars. b) The CMDs of the individual stars in both associations show that these are not evolved. c) Both associations are associated with dense CO clumps as we can see from Fig. 3. As discussed by Parker et al. (1992), these differences are indicators of age pointing towards a younger age for LH13 and 14 relative to LH9. It would be very interesting to have in the future the IMFs of LH13 and 14.

Which mechanism can initiate a second generation of stars in HII regions ? Other authors have advanced that it could be a SN explosion and that perhaps the ejection of metal rich gas at a SN explosion together with the formation of a shock front, could trigger a more massive star formation producing LH 10, 13 and 14 as a result. This would imply that the SN explosion(s) of some of the massive stars of LH 9 could have triggered this star formation (on dense molecular fragments) at the shock boundaries in a time scale of at most a few millions of years. Such a time scale is much shorter than those of previous studies trying to find evidences for this hypothesis (as for ex., in the case of Shapley Constellation III, Dopita et al. 1985). Then new questions arise. If shocks or enrichment of heavy elements are responsible for the flatter IMF of LH10, one can expect that the IMFs of LH13 and probably of LH14 should be flatter too. On the other hand, it is necessary to point out that, except for the violent motions detected in the central hole, no other evidence of SN explosions has been found in the visible or in other wavelengths. The CO clouds detected by Israel and de Graauw (1991) are distributed (Fig. 3) in a ring around LH9. They have well correlated positions with the surrounding HII regions studied in this work. Do such positions outline the borders of an old event ? Has the large molecular cloud been fragmented by the shock compression as soon as star formation started ? or has the shock front compressed the already existent molecular clumps triggering star formation inside them? Such problems will have to be examined in a larger context.

Finally it appears at the present moment the observational evidence of a type of giant bubbles that could be catalogued as "ring of HII regions" with the following distinctive characteristics:

a) Nebular diameters about 100-300 pc
b) Voids or "holes" about 100 pc in diameter
c) Large internal motions in the central hole (about 50 km s^{-1})
d) Splitting in several velocity components at the boundaries (contrary to the classical bubble expansion)
e) Thick ring of smaller HII regions, bubbles or SNRs at the boundaries
f) Association with molecular cloud complexes
g) No detection of interior X-ray emission (because of the old age of the required SNRs or wind-bubbles)

Here, we have stressed arguments that indicate that this type of "ring of HII regions" giant bubbles could be formed by sequential star formation. Only characteristics a), b), d) and sometimes f) or g) are currently available and could have led to misleading interpretations when studying giant bubbles in more distant galaxies. It seems reasonable to expect that at least some of the superbubbles (up to 1 kpc in diameter) found in several galaxies including our own Galaxy, could be formed by this type of mechanism.

Acknowledgements. M. Rosado wishes to acknowledge the invitation of the Université de Provence. This work was practically supported by the grants IN 102192 and IN 100693 of DGAPA-UNAM.

References

Amram P., Boulesteix J., Georgelin Y.P., et al.,1991, The Messenger 64, 44

Bormans D.J., de Boer K.S., Koornneef J., 1991, IAU Symp. 148, 436

Brunet J.P., Imbert M., Martin N., et al., 1975, A&AS 21, 109

Caplan J., Deharveng L., 1985, A&AS 62, 63

Chu Y.H., Kennicutt Jr. R.C., 1988, AJ 95, 1111

Danziger I.J., Liebowitz E.M., 1985, MNRAS 216, 365

Davies R.D., Elliott K.H., Meaburn J., 1976, Mem. R. Astron. Soc. 81, 89

Dopita M.A., Mathewson D.S., Ford V.L., 1985, ApJ 297, 599

Ellingsen S.P., Whiteoak J.B., Norris R.P., et al., 1994, MNRAS 269, 1019.

Georgelin Y.M., Amram P., Georgelin Y.P., et al, 1994, A&AS 108, 513

Henize K.G., 1956, ApJS 2, 315

Heydari-Malayeri M., Testor G., 1983, A&A 118, 116

Heydari-Malayeri M., Testor G., 1985, A&A 144, 98

Heydari-Malayeri M., Niemela V.S., Testor G., 1987, A&A 184, 300

Heydari-Malayeri M., Beuzit J.L., 1994, A&A 287, L17

Hodge P.W., Wright F.W., 1967, The Large Magellanic Cloud, Smithsonian Publication 4699

Hunter D.A., 1994, AJ 107, 565

Hyland A.R., Straw S., Jones T.J., Gatley I., 1992, MNRAS 257, 391

Israel F.P., de Graauw T., 1991, IAU Symp. 148, 45

Laval A., Rosado M., Boulesteix J. et al., 1992, A&A 253, 213

Le Coarer E., Amram P., Boulesteix J., et al., 1992, A&A 257, 389

Le Coarer E., Rosado M.,Georgelin Y.P., Viale A., 1993a, Proceedings of Heidelberg Conference, 15-17 Juin 1992, Second European Meeting on the Magellanic Clouds, p 77

Le Coarer E., Rosado M., Georgelin Y.P., et al. 1993b, A&A 280, 365

Lortet M.C., Testor G., 1988, A&A 194, 11

Lozinskaya T.A., 1979, A&A 71, 29

Lucke P.B., Hodge P.W., 1970, AJ 75, 171

Meaburn J., 1987, MNRAS 229, 457

Meaburn J., Mc Gee R.X., Newton L.M., 1984, MNRAS 206, 705

Meaburn J., Solomos N., Laspias V., Goudis C., 1989, A&A 225, 497

Oey M.S., Massey P., 1994, ApJ 425, 635

Parker J.W., Garmany C.D., Massey P., Walborn N.R., 1992, AJ 103, 1205

Rosado M., 1981, ApJ 250, 222

Rosado M., 1986, A&A 160, 211

Rosado M., Laval A., Boulesteix J., et al., 1990, A&A 238, 315

Sanduleak N., 1969, Cerro Tololo Interamerican Observatory, Contribution no 89

Smith A.M., Cornett R.H., Hill R.S., 1987, ApJ 320, 609

Tenorio-Tagle G., 1988, ARA&A 26, 145

Walborn N.R., Blades J.C.,1987, Ap J.323, L65

Xu C., Klein U., Meiner D., Wielebinski R., Haynes R.F., 1992, A&A 257, 47

This article was processed by the author using Springer-Verlag LaTeX A&A style file version 3.